

Natural Vibrations of Nanotubes

V. A. Eremeyev^{a, b}, E. A. Ivanova^c, Academician N. F. Morozov^d, and S. E. Strochkov^a

Received March 22, 2007

PACS numbers: 61.46.Fg, 62.20.Dc

DOI: 10.1134/S1028335807080071

Nanoobjects exhibit anomalous properties that are very attractive for applications and generally do not correlate with the properties of the macroscopic samples [1–4]. For this reason, one of the key problems of nanomechanics is the determination of the mechanical and physical characteristics of nanoobjects. One of the most efficient methods for determining elastic moduli used in the mechanics of macroobjects is based on measurement of natural frequencies.

A method for determining the natural frequencies of some nanostructures (nanotubes and nanocrystals) was proposed in [5, 6] on the basis of the measurement of natural frequencies of an “extended system” consisting of a highly oriented array (lattice) of identical nanotubes or nanocrystals, which are grown on a macroscopic substrate and are perpendicular to the substrate, and a single substrate. According to [5, 6], the spectrum of the natural frequencies of the large system can be separated into two components. One component of the system spectrum corresponds to the natural frequencies of single nanoobjects. The substrate remains almost static upon vibrations with these frequencies. The other component of the system spectrum is the spectrum of natural frequencies close to the natural frequencies of the substrate without nanoobjects. At these frequencies, the amplitude of the vibrations of the nanoobjects is much smaller than the amplitude of the substrate vibrations. Two modifications of the experimental procedure for determining the natural frequencies can be proposed in developing the method proposed in [5, 6].

Modification 1. Measure the natural frequencies of the nanotube lattice–substrate or nanocrystal lattice–substrate. Measure the natural frequencies of the same

substrate without nanoobjects. Compare the two spectra obtained. The frequencies in the system spectrum that have no correspondence among the frequencies in the substrate spectrum are the frequencies of the nanoobjects.

Modification 2. Measure the natural frequencies of the system by detecting both the electromagnetic radiation of the nanoobjects, many of which are piezoelectric materials, and the substrate vibration amplitude. The resonant frequencies at which the substrate vibration amplitude is equal to zero are the natural frequencies of the nanoobjects.

For perpendicularly oriented nanotubes, the method proposed in [5, 6] makes it possible to estimate the natural frequencies corresponding to the first natural modes of a nanotube. Using these data, it is possible to determine the rod bending stiffness of the nanotube. In order to determine the bending stiffness of the nanofilm from which the nanotube is produced, it is necessary to know the natural frequencies of the lying nanotubes. The methods for producing various nanostructures made of multilayer semiconductor nanofilms (GaAs, InAs, GeSi, etc.), which are of great interest for electronics including the electronics of nanotubes placed horizontally on the substrate, were developed in [7, 8]. The effective physical properties of such films depend significantly on their structure and residual stresses and significantly determine the durability and strength of nanostructures. The methods for investigating the bending stiffness of the nanoobjects were developed in [9, 10].

In this work, the method for determining the natural frequencies of the nanoobjects developed in [5, 6] is generalized for the nanotubes mounted in parallel to the substrate. It is shown that the several first natural frequencies corresponding to the bending vibrations of a single nanotube can be separated from the spectrum of the large system, which makes it possible to estimate their bending stiffness. The finite-element simulation of gallium arsenide nanotubes is performed.

^a Southern Scientific Center, ul. Mil’chakova 8a, Rostov-on-Don, 344090 Russia

e-mail: eremeyev@math.rsu.ru

^b Southern State University, ul. Zorge 5, Rostov-on-Don, 344090 Russia

^c St. Petersburg State Technical University, ul. Politekhnicheskaya 29, St. Petersburg, 195251 Russia

^d St. Petersburg State University, Bibliotchnaya pl. 2, Petrodvorets, St. Petersburg, 198904 Russia

ANALYTICAL ANALYSIS
OF THE MODEL PROBLEM

Let us consider a model consisting of the horizontal plate simulating the substrate and N cylindrical shells on it that simulate the nanoobjects. The plate occupies the region $0 \leq x \leq L$ and $0 \leq z \leq l$ and has the thickness H . All the shells have the same sizes (length l , radius R , and thickness h) and are located at the same distance $a = L/(N + 1)$ from each other, so that their axes are directed along the z axis. It is suggested that the shells are rigidly attached to the plate.

The basic equations of the linear shell theory have the form [11]

$$\begin{aligned} \nabla \cdot \mathbf{T} + \rho \mathbf{F} &= \rho \ddot{\mathbf{u}}, \quad \nabla \cdot \mathbf{M} + \mathbf{T}_\times + \rho \mathbf{L} = 0, \\ \mathbf{T} \cdot \mathbf{a} + \frac{1}{2}(\mathbf{M} \cdot \mathbf{b})\mathbf{c} &= {}^4\mathbf{A} \cdot \boldsymbol{\varepsilon}, \quad \mathbf{M}^T = {}^4\mathbf{C} \cdot \boldsymbol{\kappa}, \\ \boldsymbol{\varepsilon} &= \frac{1}{2}((\nabla \mathbf{u}) \cdot \mathbf{a} + \mathbf{a} \cdot (\nabla \mathbf{u})^T), \\ \boldsymbol{\kappa} &= (\nabla \boldsymbol{\varphi}) \cdot \mathbf{a} + \frac{1}{2}((\nabla \mathbf{u}) \cdot \mathbf{c})\mathbf{b}, \\ \boldsymbol{\varphi} &= -\mathbf{n} \times (\nabla \mathbf{u}) \cdot \mathbf{n}, \quad \mathbf{b} = -\nabla \mathbf{n}, \quad \mathbf{c} = -\mathbf{a} \times \mathbf{n}. \end{aligned} \tag{1}$$

Here, \mathbf{T} and \mathbf{M} are the strength and couple resultant tensors, respectively; \mathbf{T}_\times is the vector invariant of the tensor \mathbf{T} ; ρ is the surface density; \mathbf{u} is the displacement vector; $\boldsymbol{\varphi}$ is the rotation vector; $\boldsymbol{\varepsilon}$ is the tension–shear strain tensor in the tangent plane; $\boldsymbol{\kappa}$ is the bending–twisting strain tensor; ${}^4\mathbf{A}$ and ${}^4\mathbf{C}$ are the shell stiffness tensors; \mathbf{n} is the unit normal vector to the shell surface; \mathbf{a} is the unit tensor in the tangent plane; and ∇ is the surface gradient operator. To describe the bending vibrations of the cylindrical shell, we use the cylindrical coordinate system (r, θ, z) , where $r \equiv R$. Let us represent the displacement vector and rotation vector in the form of the decomposition in the cylindrical coordinate basis:

$$\mathbf{u} = u_\theta \mathbf{e}_\theta + u_z \mathbf{k} + u_r \mathbf{n}, \quad \boldsymbol{\varphi} = \varphi_\theta \mathbf{e}_\theta + \varphi_z \mathbf{k}.$$

It can be shown that the problem of the free vibrations of the shell described by Eqs. (1), which correspond to the lowest natural frequencies, reduces to the differential equation

$$\frac{D}{\rho R^4} \frac{d^2}{d\theta^2} \left(\frac{d^2}{d\theta^2} + 1 \right)^2 u_r + \left(\frac{d^2}{d\theta^2} - 1 \right) \ddot{u}_r = 0, \tag{2}$$

where D is the bending stiffness of the shell.

Solutions of Eq. (2) have the form $u_r(\theta, t) = U_r(\theta)e^{i\omega t}$, where

$$U_r(\theta) = \sum_{j=1}^3 [A_j \sin(\lambda_j \theta) + B_j \cos(\lambda_j \theta)].$$

Here, λ_j is the roots of the characteristic equation

$$\lambda^6 - 2\lambda^4 + (1 - \Omega^2)\lambda^2 - \Omega^2 = 0, \text{ where } \left(\Omega = \omega \sqrt{\frac{\rho}{D}} R^2 \right),$$

and the integration constants A_j and B_j are determined from the periodicity conditions

$$\begin{aligned} u_\theta(0, t) &= u_\theta(2\pi, t), \quad u_r(0, t) = u_r(2\pi, t), \\ \varphi_z(0, t) &= \varphi_z(2\pi, t) \end{aligned}$$

and the conditions of the matching of the shell with the substrate.

The bending vibrations of the plate are described by the equations

$$\begin{aligned} \nabla \cdot \mathbf{T} + \sum_{n=1}^N \mathbf{F}_n \delta(x - na) &= \rho_* \ddot{\mathbf{u}}, \\ \nabla \cdot \mathbf{M} + \mathbf{T}_\times + \sum_{n=1}^N \mathbf{L}_n \delta(x - na) &= 0, \end{aligned} \tag{3}$$

where $\mathbf{F}_n = \mathbf{e}_\theta \cdot \mathbf{T}^{(n)}|_{\theta=0}$ and $\mathbf{L}_n = \mathbf{e}_\theta \cdot \mathbf{M}^{(n)}|_{\theta=0}$ are the force and couple acting on the plate by the n th cylindrical shell and $\delta(x)$ is the Dirac delta function. Disregarding the transverse shear strain and tension of the plate, one can reduce the equation of motion (3) to the form

$$\begin{aligned} C \Delta \Delta w + \rho_* \ddot{w} &= - \sum_{n=1}^N (T_{\theta r}^{(n)}|_{\theta=0} \delta(x - na) \\ &+ M_{\theta z}^{(n)}|_{\theta=0} \delta'(x - na)), \end{aligned} \tag{4}$$

where w is the transverse bending (displacement in the y direction), C is the bending stiffness of the plate, and ρ_* is the surface density of the plate. The solutions of Eq. (4) are sought in the form $w(x, z, t) = W(x, z)e^{i\omega t}$.

Analysis of the equations determining the integration constants $A_j^{(n)}$, and $B_j^{(n)}$, $n = 1, 2, \dots, N$, shows that two alternative situations are possible.

1. In the first case, nontrivial solutions exist if

$$W|_{x=na} = 0, \quad W'|_{x=na} = 0. \tag{5}$$

Since the sizes of the shells simulating the nanoobjects are much smaller than the sizes of the plate simulating the substrate and the number of the shells is large, it is possible to suggest that the shells are continuously distributed over the plate surface. In this case, discrete conditions (5) are changed to the continuous conditions

$$W(x) \equiv 0, \quad W'(x) \equiv 0 \left(W' \equiv \frac{\partial W}{\partial x} \right).$$

Under these conditions, the plate is at rest. Such solutions describe the vibrations of the cylindrical shells lying on a rigid foundation. Thus, the spectrum of the natural frequencies of the nanoobjects is separated from the system spectrum.

2. In the second case, the substrate undergoes vibrations together with the nanotubes. It can be shown that

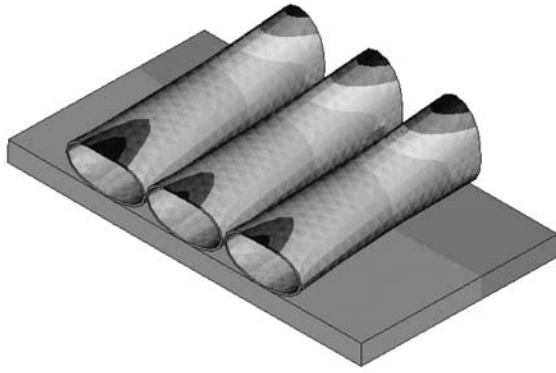


Fig. 1. Natural modes localized in nanotubes.

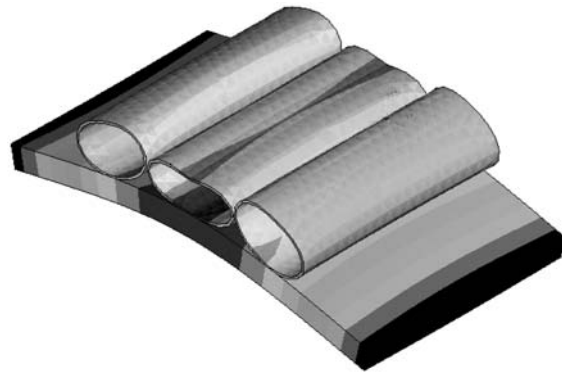


Fig. 2. Natural mode corresponding to the first bending mode of the substrate.

the smallness of the dynamic terms associated with the presence of nanoshells is determined exclusively by the smallness of the sizes of the shells as compared to the plate sizes. For the force factors determined by the shells to be small, the shell thickness must be much smaller than the plate thickness and the linear sizes of the plate and shells must differ not so strongly. The smallness of the quantity $N\left(\frac{h}{N}\right)^3\left(\frac{L}{R}\right)^2$ is decisive.

The behavior of the system with horizontally located nanotubes differs from the behavior of a similar system with vertically located nanotubes [5, 6], because the horizontally attached nanotubes change the effective stiffness of the plate and the plate with the horizontal nanotubes is effectively anisotropic and inhomogeneous.

NUMERICAL ANALYSIS OF THE NATURAL OSCILLATIONS

For an arbitrary form of the stress–strain state, we investigate the system consisting of a certain number of nanotubes lying parallel to each other on the substrate in the framework of three-dimensional theory by means of the finite-element method. Since the materials under consideration (GaAs, InAs, GeSi, etc.) have piezoelectric properties [12, 13], this system as a whole is a composite piezoelectric body. In the electrostatic approximation in the absence of mass forces, the electroelasticity equations have the form [14]

$$\rho \ddot{\mathbf{u}} = \nabla \cdot \boldsymbol{\sigma}, \quad \nabla \cdot \mathbf{D} = 0, \quad (6)$$

$$\boldsymbol{\sigma} = \mathbf{C} \cdot \boldsymbol{\varepsilon} - \mathbf{e} \cdot \mathbf{E}, \quad \mathbf{D} = \mathbf{e} \cdot \boldsymbol{\varepsilon} + \boldsymbol{\varepsilon} \cdot \mathbf{E}, \quad (7)$$

$$\boldsymbol{\varepsilon} = \frac{1}{2}(\nabla \mathbf{u} + \nabla \mathbf{u}^T), \quad \mathbf{E} = -\nabla \varphi, \quad (8)$$

$$\begin{aligned} \mathbf{u}|_{\Gamma_1} &= \mathbf{u}_0, & \mathbf{n} \cdot \boldsymbol{\sigma}|_{\Gamma_2} &= \mathbf{f}, & \varphi|_{\Gamma_3} &= \varphi_0, \\ \mathbf{n} \cdot \mathbf{D}|_{\Gamma_4} &= q. \end{aligned} \quad (9)$$

Here, \mathbf{u} is the displacement vector, \mathbf{E} is the electric field strength, φ is the electric potential, $\boldsymbol{\sigma}$ is the stress tensor, \mathbf{D} is the electric induction vector, $\boldsymbol{\varepsilon}$ is the strain tensor, ∇ is the three-dimensional gradient operator, ρ is the density, \mathbf{C} is the stiffness matrix, \mathbf{e} is the piezoelectric constant, and $\boldsymbol{\varepsilon}$ is the dielectric constant. The displacements \mathbf{u}_0 are specified on the part Γ_1 of the body boundary Γ , the forces \mathbf{f} are specified on the part Γ_2 , the electric potential φ_0 is specified on the part Γ_3 , and the surface charge q is specified on the part Γ_4 ($\Gamma = \Gamma_1 \cup \Gamma_2 = \Gamma_3 \cup \Gamma_4$, $\Gamma_1 \cap \Gamma_2 = \emptyset$, $\Gamma_3 \cap \Gamma_4 = \emptyset$).

For the modal analysis of the boundary value problem specified by Eqs. (6)–(9), we use the ANSYS finite-element analysis software. A number of numerical experiments are performed for various numbers of the nanotubes (from one to ten), various system geometries (the ratio of the thicknesses of the substrate and nanofilm, the ratio of the nanotube radius to the substrate length, etc.), and various substrate attachment conditions. We consider the materials of the substrate and nanotubes used in applications [7]; the properties of these materials are taken from [12, 13], and the geometrical parameters are taken from [7, 8]. The calculations show that, for any attachment of the substrate, it is possible to choose the problem parameters such that the natural frequencies of the nanotubes and substrate can be extracted from the general spectrum of the large system. This numerically confirms the results of the above theoretical analysis.

The calculation results for the free sapphire substrate with three GaAs nanotubes are shown in Figs. 1–4. Figures 1–3 show certain natural modes, and Fig. 4 shows the distribution of the natural frequencies over their ordinal numbers. The squares in Fig. 4 are the modes at which significant motions of the substrate are observed, whereas the circles are the natural frequencies at which the substrate is almost at rest and the nanotubes oscillate. Figure 1 corresponds to the natural vibrations localized in the nanotubes. The natural frequencies of these vibrations (the first six points in Fig. 4) correspond to the first natural frequency of the nano-



Fig. 3. Example of a high-frequency natural mode: vibrations of the substrate and nanotubes.

tube mounted on a part of the lateral surface. At these frequencies, the substrate is almost at rest, whereas the nanotubes undergo vibrations at which their cross section becomes elliptic. These first frequencies make it possible to estimate the bending stiffness of the film forming the nanotube. Figure 2 shows the natural vibrations at the frequency corresponding to the first bending mode of the substrate vibrations. In contrast to [5, 6], where the vertically mounted nanoobjects in these modes move almost as absolutely rigid bodies, this vibration mode is also accompanied by the deformation of the nanotubes in this case.

Note that the interaction between the substrate and nanotubes in the vibrations is stronger than that for the case of the vertical array of nanocrystals [5, 6]. Figure 3 shows the mode at which the substrate oscillates with the third natural frequency (the last point in Fig. 4); at the same time, the form of the vibrations of the nanotubes corresponds to the high-frequency vibrations of a single nanotube. Since the distributed nanotubes affect not only the total system mass, but also its effective stiffness, not only is the form of the vibration modes shown in Fig. 3 different, the natural frequencies of the large system also differ from the natural frequencies of both the free substrate and the single nanotube. For the first frequencies, the numerical coincidence of the natural frequencies of the large system with the respective partial natural frequencies of the substrate and single nanotube is satisfactory.

The numerical analysis also shows the presence of natural vibrations localized in a single nanotube. Such vibrations are less interesting for detection in the experiments, particularly in the case of measurement of the appearing electric fields, because the field strength increases with the number of oscillating nanotubes. Thus, the efficiency of the proposed method increases with the number of nanotubes on the substrate.

The finite-element calculations in the framework of the three-dimensional theory confirm the conclusion made above on the basis of the analysis of the two-dimensional equations of motion of the shell that the

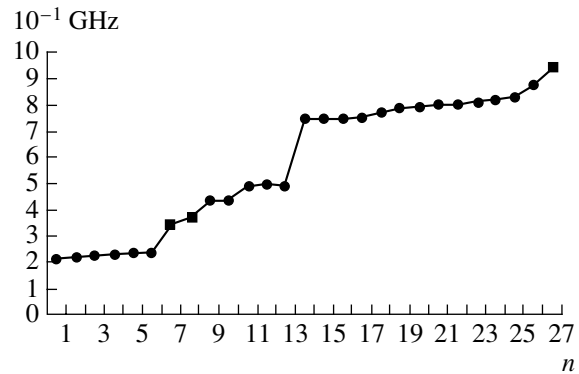


Fig. 4. Distribution of the natural frequencies of the large system vs. their number n . The squares are the natural frequencies corresponding to the vibrations of the substrate.

natural frequencies of the single nanotube can be separated. The above theoretical and numerical analysis provides the conclusion that the natural frequencies of the nanotube can be experimentally determined on the basis of the proposed modifications.

ACKNOWLEDGMENTS

This work was supported by the Russian Foundation for Basic Research (project nos. 05-01-00094-a and 06-000452-a), by the Russian Science Support Foundation, and by the Council of the President of the Russian Federation for Support of Young Scientists and Leading Scientific Schools (project nos. MD-4829.2007.1 and NSh-4518.2006.1).

REFERENCES

1. M. Yu. Gutkin and I. A. Ovid'ko, *Defects and Mechanisms of Plasticity in Nanostructural and Noncrystalline Materials* (Yanus, St. Petersburg, 2003) [in Russian].
2. A. M. Krivtsov and N. F. Morozov, Dokl. Phys. **46**, 825 (2001) [Dokl. Akad. Nauk **381**, 345 (2001)].
3. *Springer Handbook of Nanotechnology*, Ed. by B. Bhushan (Springer, Berlin, 2004), Vol. 36.
4. *Handbook of Nanoscience, Engineering, and Technology*, Ed. by W. A. Goddard, D. W. Brenner, and S. E. Lyshevski (CRC, Boca Raton, 2003).
5. V. A. Eremeyev, E. A. Ivanova, N. F. Morozov, and A. N. Solov'ev, Dokl. Phys. **51**, 93 (2006) [Dokl. Akad. Nauk **406**, 756 (2006)].
6. V. A. Eremeyev, E. A. Ivanova, N. F. Morozov, and A. N. Solov'ev, Tech. Phys. **52**, 1 (2007) [Zh. Tekh. Fiz. **77**, 3 (2007)].
7. S. V. Golod, V. Ya. Prinz, V. I. Mashanov, and A. K. Gutakovski, *Semicond. Sci. Technol.* **16**, 181 (2001).
8. V. Ya. Prints and S. V. Golod, Prikl. Mekh. Tekh. Fiz., No. 6, 114 (2006).
9. E. A. Ivanova, A. M. Krivtsov, and N. F. Morozov, Dokl. Phys. **47**, 620 (2002) [Dokl. Akad. Nauk **385**, 494 (2002)].

10. E. A. Ivanova and N. F. Morozov, *Dokl. Phys.* **50**, 83 (2005) [*Dokl. Akad. Nauk* **400**, 475 (2005)].
11. P. A. Zhilin, *Applied Mechanics. Fundamentals of Theory of Shells* (Politekh. Univ., St. Petersburg, 2006) [in Russian].
12. A. A. Blistanov, V. S. Bondarenko, N. V. Perelomova, F. N. Strizhevskaya, V. V. Chkalova, and M. N. Shaskol'skaya, *Acoustic Crystals* (Nauka, Moscow, 1982) [in Russian].
13. A. Dargys and J. Kundrotas, *Handbook of Physical Properties of Ge, Si, GaAs, and InP* (Sci. and Encyclopedia, Vilnius, 1994).
14. G. A. Maugin, *Continuum Mechanics of Electromagnetic Solids* (North-Holland, Amsterdam, 1988; Mir, Moscow, 1991) [in Russian].

Translated by R. Tyapaev